

# Differential and average approaches to Rose and Mei dropwise condensation models

Solmaz Boroomandi Barati\*, Jean-Charls Pinoli†, Stéphane Valette‡ and Yann Gavet §

**Abstract**—Two well-known models for drop-size distribution function during dropwise condensation -called Rose model and Mei model- were examined in two different aspects, average and differential point of view. It has been proved that these two models are able to describe the relation between droplets size and distribution function at each time step. The goal of this research is to investigate how these models can predict the relation between average distribution function ( $N_{ave}$ ) and average radius ( $r_{ave}$ ) of droplets during a complete procedure of dropwise condensation and the relation between differential distribution function ( $\frac{dN}{dr}$ ) and drops radius ( $r$ ) at each time step. The empirical parameters are drop size distribution exponent ( $n$ ) and fractal dimension ( $df$ ) in Rose model and Mei model respectively. At first these two parameters were calculated based on the experimental data and then the validity of these calculations for our computer simulation was investigated. It was concluded that Rose method fits the results of differential distribution function with exponent  $n$  between 0.33 and 0.35, and average distribution function with  $n$  of around 0.38. The Mei model also can describe both differential and average results of simulation and experiments with fractal dimension of  $1.79 < df < 1.99$ . Also it was observed that the value of both  $n$  and  $df$  vary with changing the ratio of radius of two following droplets generation ( $\gamma$ ) in our computer simulation.

**Index Terms**—dropwise condensation, fractal geometry, drop-size distribution function, Mei method, Rose method.

## I. INTRODUCTION

**D**ROPWISE condensation has been in the center of concentration during last few decades due to its higher heat transfer coefficient with respect to filmwise condensation. It was said that heat transfer coefficient of filmwise condensation is about 5 to 7 times smaller than in dropwise condensation [1]. Generally dropwise condensation includes five main steps: nucleation of initial droplets, growth due to adsorption, growth due to coalescence, nucleation of new droplets, and sliding of very big drops (that was not considered here). The result of the last three stages is the change in number

of droplets as well as their size. One can consider drop-size distribution function ( $N$ ) as the cumulative number of droplets bigger than a specified value per unit area (or per unit area and size). It is obvious that both coalescence and nucleation of new droplets change  $N$  during dropwise condensation.

Changes of  $N$  with respect to droplets radius ( $r$ ) attracted lots of attention specially, after the works of Rose and his colleagues during 1990s. Le Fevre and Rose [2] were the first ones who were able to describe  $N$  successfully and their model was used by a lot of scientists up to now. Then, Rose and Glicksman [3] derived a power law model to describe the relation between  $N$  and  $r$  as well. To investigate time-series features and the percentage of surface occupied by droplets, Tanaka [4] numerically solved two equations relating to the spatial distribution of droplets. Tanasawa and Ochiai [5] also derived an empirical distribution function and conducted a huge amount of experiments and numerical investigations on dropwise condensation. More recently Mei et al. [6], [7] developed a fractal model based on fractal geometry theory. They supposed that since the pictures taken at different scales from droplets during dropwise condensation are the same, the droplets will follow the law of fractal geometry theory. The importance of their work is due to describing  $N$  by parameters that have physical meanings, such as droplets surface fraction, fractal dimension of droplets pattern, and the maximum radius of droplets. Baojin and his colleagues [1] developed the Rose model for all contact angles considering contact angle hysteresis to be able to describe droplets growth in both hydrophobic and hydrophilic surfaces. Wu et al. [8] introduced an algorithm to generate droplets based on the Rose model and calculate the rate of heat transfer based on this algorithm. At last, Watanabe et al. [9] investigated the results of all these methods with their experimental data.

Although lots of works have been done up to now for describing  $N$  in dropwise condensation, two interesting aspects of this process remained still unclear: differential and average distribution function. Differential distribution function ( $\frac{dN}{dr}$ ) represents the differential changes in drop-size distribution function and average distribution function ( $N_{ave}$ ) deals with total number of droplets divided by total area and average radius of droplets ( $r_{ave}$ ) at each time step. More precisely,

\*S. Boroomandi Barati is with Univ Lyon, Ecole Nationale Supérieure des Mines de Saint-Etienne, LGF UMR CNRS 5307, SAINT-ETIENNE, France, e-mail: (solmaz.boroomandi@emse.fr).

†J.-C. Pinoli is with Ecole Nationale Supérieure des Mines de Saint-Etienne, LGF UMR CNRS 5307, SAINT-ETIENNE, France.

‡S. Valette is with Univ Lyon, Ecole Centrale de Lyon, LTDS UMR CNRS 5513, F-69134, LYON, France.

§Y. Gavet is with Ecole Nationale Supérieure des Mines de Saint-Etienne, LGF UMR CNRS 5307, SAINT-ETIENNE, France.

almost all of the scientific publications deal with the relation between  $N$  and  $r$  at each time step, but the relationship between  $N_{ave}$  versus  $r_{ave}$  and  $\frac{dN}{dr}$  versus  $r$  was not clearly discussed up to now.

In this research we are going to introduce these two different approaches towards dropwise condensation modeling and apply them to Rose and Mei models. In this regard at first a series of experiments were conducted and the images were taken from droplets at  $\Delta T = 1s$ . These images were binarized and used to measure experimental parameters. Then we used a fractal generating algorithm to produce different generations of droplets in computer simulation. The results of experiments and simulation are compared with theory according to the two mentioned aspects. Considering these two aspects for each of the theoretical formulas, we will represent four linear equations as below

- 1) Differential Rose method, describing evolution of  $\frac{dN}{dr}$  with respect to  $r$  at each time step
- 2) Average Rose method, describing evolution of  $N_{ave}$  based on  $r_{ave}$  during the whole process time
- 3) Differential Mei method, describing evolution of  $\frac{dN}{dr}$  with respect to  $r$  at each time step
- 4) Average Mei method, describing evolution of  $N_{ave}$  based on  $r_{ave}$  during the whole process time

#### A. Rose Method [3]

This method is cited as empirical or Rose method in the specialized literature and is based on the sequence of events occurring during the growth cycle. Rose [3] used a power law model to describe the total area ( $A$ ) covered by droplets with radius greater than a specified value of  $r$ .

$$A = 1 - \left(\frac{r}{r_{max}}\right)^n \quad (1)$$

where  $n$  is an empirical parameter known as the drop size distribution exponent and must be determined experimentally. Rose and Glicksman [3] reported  $n = 0.382$  based on the theoretical evidences. Wu [8], [6] assumed  $n = \frac{1}{3}$  based on the experimental works of Graham and Griffith [10] and Tanaka [11] that reported  $n$  laying in the real number range [0.313-0.350]. Mei[6] also used  $n = \frac{1}{3}$  based on experimental results of other researchers. The most frequently reported value for  $n$  in literature is around  $\frac{1}{3} = 0.33$ . Maximum radius of each generation of droplets before sliding ( $r_{max}$ ) can be derived by force balance between surface tension and droplet weight and for hemisphere droplets is [12]:

$$r_{max} = \sqrt{\frac{3\sigma}{(\rho_l - \rho_v)g}} \quad (2)$$

where  $\sigma$  is liquid surface tension,  $\rho_l$  and  $\rho_v$  are liquid and vapor density respectively, and  $g$  is earth

acceleration. If we consider  $N$  as the number of drops per unit size which have radius greater than  $r$ , then the differential distribution function of droplets size will be as below:

$$f(r) = \frac{-dN}{dr} = \frac{-1}{\pi r^2} \frac{dA}{dr} = \frac{n}{\pi r_{max}^3} \left(\frac{r}{r_{max}}\right)^{(n-3)} \quad (3)$$

Most of the time the logarithmic version of this equation is used to describe the spatial distribution pattern of droplets:

$$\log\left(\frac{-dN}{dr} r_{max}^3\right) = \log\left(\frac{n}{\pi}\right) + (n-3)\log\left(\frac{r}{r_{max}}\right) \quad (4)$$

The logarithmic scale is more preferable because the terms are dimensionless and thus easier to compare. Moreover droplets nucleation function is normalized for size of droplets and area of fractal zone and thus the results will be independent of experimental situation. From equation 3, if we consider  $N$  as the total number of droplets of each generation per unit area and unit radius, the time average version of Rose method will be [6]:

$$\log(N_{ave}) = \log\left(\frac{n}{\pi}\right) - n\log(r_{max}) + (n-3)\log(r_{ave}) \quad (5)$$

where  $r_{ave}$  here is the average radius of droplets of each generation. Equations 4 and 5 represent differential and average Rose method, respectively. It has been frequently said that if we take pictures of droplets at different scales over time or space, all of them are similar and follow the same spatial pattern. This is known as the rule of self-similarity. According to the concept of self-similarity, we can say that droplet size distribution obeys the same rule in all size ranges and this is apparent by comparing equations 4 and 5.

#### B. Mei Method [6], [7]

The second method applied to describe dropwise condensation based on fractal units comes from the fractal geometry theory. According to this theory, in a fractal zone if we assume the size of the biggest particle equal to  $l_{max}$  made up of smaller units with size of  $l$ , the number of fractal units bigger than  $l$  is [13]:

$$N = \left(\frac{l_{max}}{l}\right)^{d_f} \quad (6)$$

$$d_f = \lim_{r \rightarrow 0} \frac{\log(N)}{\log\left(\frac{r_{max}}{r}\right)} \quad (7)$$

where  $d_f$  is the fractal dimension and is different for each of fractal patterns. For 2-dimensional droplets growing on a flat surface  $d_f$  is smaller than 2, while for 3-dimensional ones  $d_f$  is smaller than 3 [7]. Based

on fractal geometry theory, the cumulative number of droplets bigger than a specified value of  $r$  on a flat surface during dropwise condensation is:

$$N = \left(\frac{r_{max}}{r}\right)^{d_f}, \quad \text{for } r_{min} < r < r_{max} \quad (8)$$

By differentiating from equation 8 with respect to  $r$ , the differential distribution function of droplets size will be:

$$f(r) = \frac{-dN}{dr} = \frac{d_f}{r_{max}} \left(\frac{r_{max}}{r}\right)^{d_f+1} \quad (9)$$

The negative sign indicates opposite relation between size and number of droplets. Equation 9 in log-log system is a straight line with slope and intercepts that are function of  $d_f$ :

$$\log\left(r_{max} \frac{-dN}{dr}\right) = \log(d_f) - (d_f+1)\log\left(\frac{r}{r_{max}}\right) \quad (10)$$

To be able to derive an average model comparable with equation 5, this equation must be divided by the total area occupied by fractal particles. Total area of a fractal zone was calculated by Mei [6] by integrating equation 10 :

$$A = \int_{r_{min}}^{r_{max}} -dN \pi r^2 = \frac{\pi d_f (1-\phi) r_{max}^2}{(2-d_f)\phi} \quad (11)$$

where  $\phi$  is the fraction of covered area by a fractal zone and is equal to:

$$\phi = \left(\frac{r_{min}}{r_{max}}\right)^{2-d_f} \quad (12)$$

where  $r_{min}$  is the size of the smallest viable droplets and must be calculated based on physical evidences [14]:

$$r_{min} = \frac{(2\sigma T_s)}{H_{fg}\rho(\Delta T_t)} \quad (13)$$

It is obvious that  $r_{min}$  is just a function of the process conditions and physical properties of liquid. Dividing equation 9 by equation 11 and next taking logarithm, we will get the average distribution function of droplets for Mei model:

$$\log(N_{ave}) = \log\left(\frac{(2-d_f)\phi}{\pi(1-\phi)}\right) + (d_f-2)\log(r_{max}) - (d_f+1)\log(r_{ave}) \quad (14)$$

This equation represents a straight line with slop and intercept as functions of  $d_f$  and surface coverage( $\phi$ ). Both of these parameters are depended on temperature difference between cold substrate and hot air. Equations 10 and 14 are differential and average Mei distribution of droplets during dropwise condensation. These two

formulas are based on the fractal geometry theory and assume the droplets as fractal particles growing in a fractal zone with area equal to equation 11.

## II. EXPERIMENTAL APPARATUS

Experimental setup consists of a chamber containing hot air and cold substrate and a compressor to adjust relative humidity about 40 percent inside the chamber. Temperature of hot air is set to  $86^\circ F$ , while substrate temperature is around  $62^\circ F$ . Nucleation and growth of droplets are recorded by a high resolution CCD camera installed outside the chamber in time intervals of 1s. The images taken by CCD camera then are binarized and used to model droplets nucleation and growth.

## III. FRACTAL SIMULATION ALGORITHM

Present simulation develops the model proposed by Wu et al. [8] both in time and space domains. According to this model the square substrate with length  $l$  is divided iteratively to  $\gamma^2$  small squares and  $p$  percent of these small squares are chosen completely randomly as new generation droplets. The idea behind this simulation is indicated in figure 1.

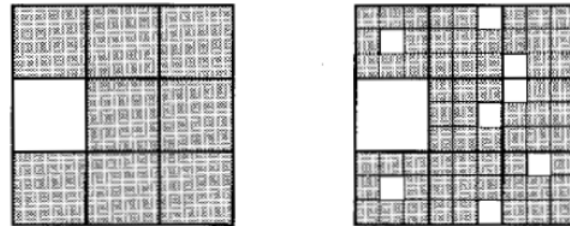


Figure 1. Illustration of how to generate droplets of each generation in fractal simulation algorithm ( $\gamma = 3$ )

In other words consider a square of length 1. At the first step each side of this square is divided to  $\gamma$ , so now there are  $\gamma^2$  small squares in the whole area. If we consider  $p$  as the fraction of available area for each generation of droplets, in the first step  $p \times \gamma^2$  small squares must be randomly chosen as the first generation droplets. The choice of droplets was done based on Poisson point process, which generates completely random spatial distribution of points in the whole domain. In the second step each length of each small squares is divided by  $\gamma$  again and  $p$  percent of resulted squares are chosen as the second generation of droplets. This process continues till reaching the size of smallest viable droplets.

The fraction of available area  $p$  is the same for all generations and can be referred to as the probability of finding a droplet in a elementary square at each step. At each step, the chosen squares are assumed as hemispherical droplets so a correction factor equal to  $p = p \times \pi/4$  must be considered in calculations. Procedure of generating random droplets of each generation is shown in figure 2. Although for generation

$k$  available area is fewer than generation  $k - 1$ , since there are more squares available to find droplets, there are more droplets in generation  $k$  with respect to  $k - 1$ . In the other words, in each generation available area reduces, while number of droplets increase because droplets are smaller and need smaller amount of area to locate. This is the concept of linear relation between  $\log(N)$  and  $\log(r)$  during time. Analysis of droplets nucleation and growth was carried out based on each image at steady state time as well as based on average parameters during procedure.

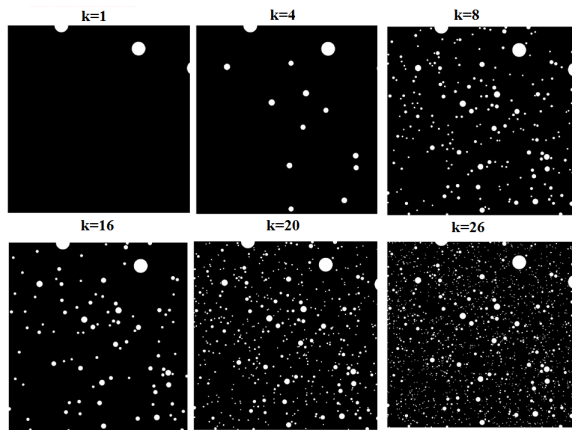


Figure 2. Illustration of generating random droplets, whose centers obey Poisson spatial point process in 6 different generations,  $k = 1, 4, 8, 16, 20, 26$ . At first the biggest droplets are formed by dividing substrate in to  $\gamma^2$  squares and choosing  $p$  percent of them completely randomly. Then in each step smaller droplets are generated with the same pattern.

The droplets are located one by one to avoid any overlap between them. In reality, if a pair of droplets touch each other they will coalesce and form a bigger drop in their mass center. Thus, in the current method the droplets are added one by one and for each droplets there is a check to insure that the cell is not occupied by another droplets.

#### IV. RESULTS AND DISCUSSION

##### A. Model Validation, Comparison With Experimental Results

Figures 3 and 4 compare the results of equations 4 and 10 with data obtained from experiments, at different time intervals. In these two figures Rose and Mei models are calculated for experiments of  $t = 60s$  and  $t = 100s$ . The time intervals were chosen after starting coalescence in order to have both adsorbing - or small- and coalescence -or big- drops. The concept of small and big droplets comes from the critical radius ( $r_c$ ), which was introduced as the half-spacing between active sites on substrate [15]. For square substrate with  $A = L \times L$  it will be:

$$r_c = \sqrt{\frac{L^2}{4\hat{N}}} \quad (15)$$

where  $\hat{N}$  here is the number of droplets. Droplets smaller than  $r_c$  grow mainly due to adsorbing water molecules from humid air, while the main reason of growth of droplets bigger than  $r_c$  is coalescence. Figure 3 shows good agreement between experimental results and differential Rose model with  $n$  between 0.33 and 0.35, especially for bigger droplets. The same deviations near small drops was described before by Wu et al. [8] and Baojin et al. [1] while studying experimental results of dropwise condensation. Due to deviation around small droplets Rose method usually introduces as a method to describing evolution of coalescing droplets. Obtaining  $r_{max}$  from equation 2 and  $r_c$  from equation 15, we will have  $-1.9 < \log \frac{r_c}{r_{max}} < -2.9$  -depending on the experiment time- that is exactly the point after which the deviations from straight line start in figure 3. So, it can be claimed that equation 4 that has been used before, to describe  $N$ , has also a good understanding of  $\frac{dN}{dr}$ , especially for droplets bigger than  $r_c$ .

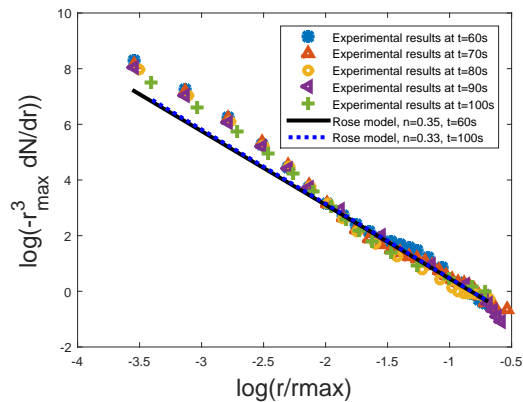


Figure 3. Comparison of the results of Rose model (equation 4) and experimental results at 5 different steps of  $t = 60, 70, 80, 90, 100s$ .

Figure 4 shows acceptable agreement between experimental results and equation 10 with  $df$  between 1.79 - 1.99 in all time intervals. The deviations around very small and very big droplets were observed by Mei himself [16]. For very small and very big droplets the number of droplets depends on the physical properties of process like contact angle hysteresis and starvation of substrate for growing small droplets in vacant area around bigger ones. So, these deviations maybe seen frequently.

The predicted results for  $N_{ave}$  by Rose method (equation 5) and Mei method (equation 14) is presented in figure 5 as well as experimental results. This figure highlights that experimental  $N_{ave}$ s are fitted by the two models very well with  $n = 0.38$  and  $df = 1.99$ . Figure 5 shows that both Rose and Mei methods can describe droplets growth by adsorption and coalescence from minimum to maximum radius. Also, it can be said that according to this figure droplets nucleation and growth during the whole process from  $r_{min}$  to  $r_{max}$  obeys the same pattern in which fractal particles grow.

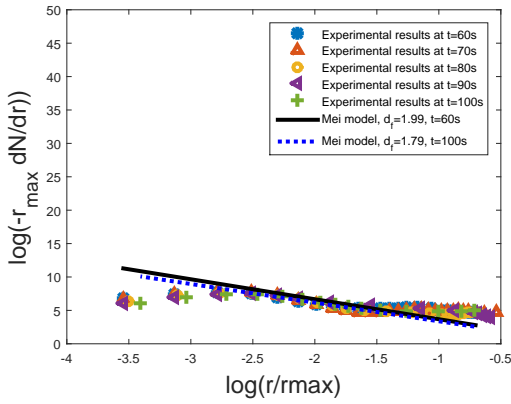


Figure 4. Comparison of the results of MeI model (equation 10) and experimental results at 5 different steps of  $t = 60, 70, 80, 90, 100s$ .

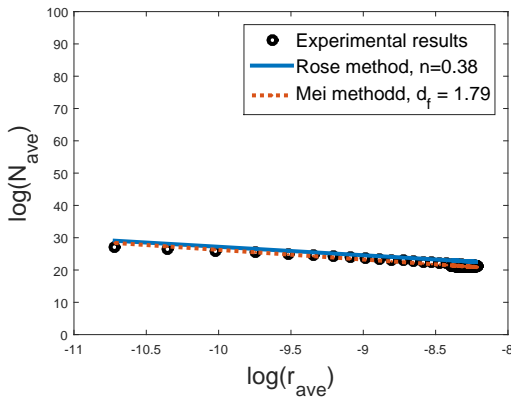


Figure 5. Comparison of the results of average Rose model (equation 5) and average MeI model (equation 14) with experimental results.

*B. Examination Simulation Procedure With The Two Methods*

Comparison of the results from simulation with the two models are presented in figure 6. It can be seen that predicted line of differential MeI model fits the simulation results with  $df = 1.99$ , while the line of differential Rose model fits them with  $n = 0.35$ . These values for  $n$  and  $df$  agree very well with experimental results discussed in section IV-A. Figure 7 also shows that both average MeI and Rose models fit simulation results with  $n = 0.38$  and  $df = 1.79$ . The surprisingly good agreement between simulation and predicted values from both differential and average models with expected values of  $n$  and  $df$  validates the method that was used for simulating dropwise condensation. All of these graphs indicate that the process of dropwise condensation obeys the rule of fractals in both differential and average scales.

It is worth to point out here that the grid number is an important parameter in simulation that can affect the values of  $n$  and  $df$ . Grid number refers to the number of small squares in each iteration from which the number of droplets are chosen. So, it has a direct influence on the distribution function of each generation of

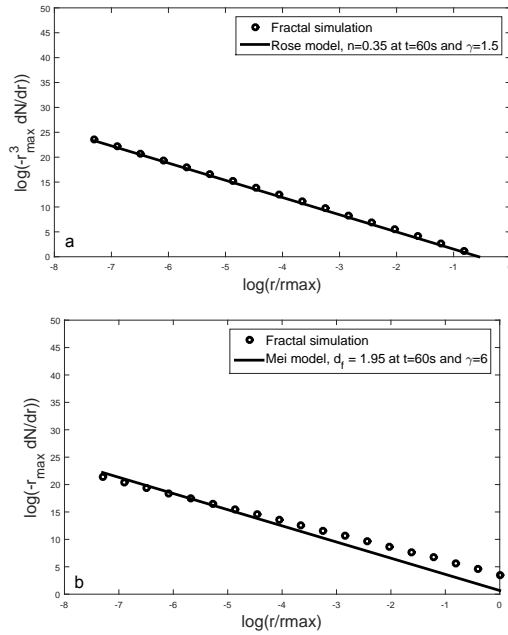


Figure 6. Comparison of the results of both models and results from fractal simulation (a) Rose model(equation 4) (b) MeI model (equation 10).

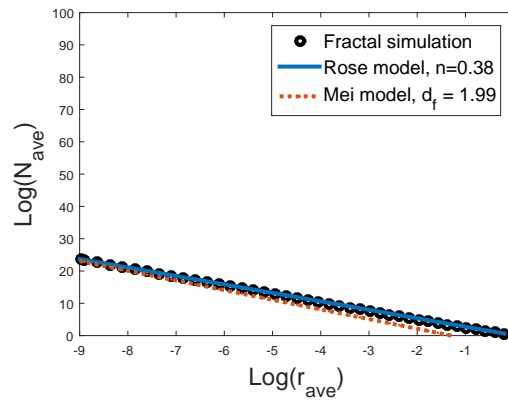


Figure 7. Comparison of the results of average Rose model (equation 5) and average MeI model (equation 14) with results from fractal simulation

droplets. For simplification, instead of grid number we can investigate the effect of  $\gamma$  that is the side length reduction coefficient in each step.

$$\frac{1}{\gamma} = \frac{r_{k+1}}{r_k} \tag{16}$$

Whit this definition the grid number will be  $\gamma^2$ . Choosing bigger values for  $\gamma$  will lead to smaller size but higher number of droplets in each generation (bigger  $\gamma$ , smaller  $r$ , bigger  $N$ ). This will change the values of both right and left hand sides of equations 4 and 10 and changes in both parameters  $n$  and  $df$ . Figure 8 shows that by increasing  $\gamma$  the slope of both lines of equations 4 and 10 increase but the intercept does not

change significantly. This is because intercept of both lines are in log scale ( $\log(\frac{n}{\pi})$  and  $\log(df)$ ) and are not sensible enough to show the changes. From these two graphs, it is expected to see the sharp increase in both  $n$  and  $df$ .

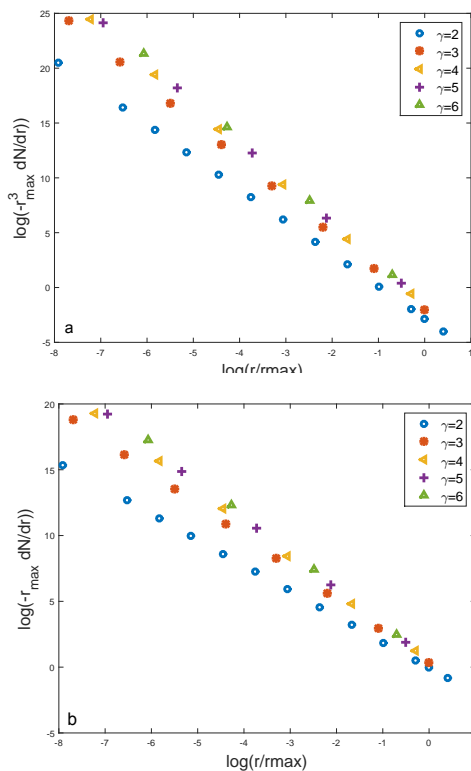


Figure 8. Results of both methods at different  $\gamma$  (a) Rose model (b) Mei model

The predictions for increase in  $n$  and  $df$  are supported by figure 9. According to this figure, increase in  $\gamma$  will lead to a jump in the value of  $n$  and then a constant trend around 0.75. The same pattern is apparent in figure 9 (b), for  $df$  that increases rapidly from 0.9 to 1.99 by changing  $\gamma$  from 2 to 6. These figures indicate that the accuracy of simulation proposed in section III depends on the value of  $\gamma$ . Depending on the value of  $\gamma$   $n$  can vary from 0.04 to around 0.75 and the most reported value that is  $n = 0.33$  can be obtained by  $\gamma = 2.5$ . In the case of differential Mei method  $df$  varies from 0.9 to 1.99 and the best value that is 1.99 is calculated with  $\gamma = 6$ .

## V. CONCLUSION

The aim of this research was to investigate drop-size distribution function of droplets during dropwise condensation in both differential and average scales. In this regard, two sets of data were extracted from experimental set up and from our computer simulation algorithm. The models used here were Rose and Mei models that have powerful theoretical basis. It was concluded that both differential and average Rose models were able to describe coalescing droplets evolution with exponent ( $n$ ) between 0.33 and 0.35 and 0.38

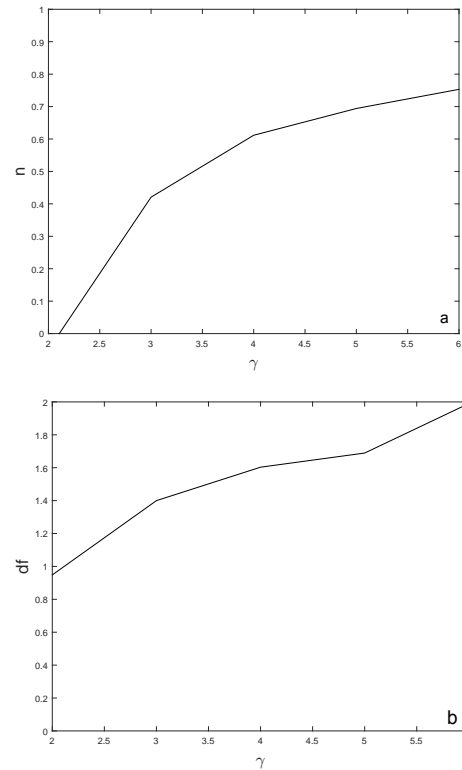


Figure 9. (a)  $n$  v.s  $\gamma$  (b)  $df$  v.s  $\gamma$

respectively. While for differential and average Mei models the important parameter is fractal dimension ( $df$ ) and was between 1.79-1.99 for both experimental and simulation data. Also the effect of side length reduction coefficient ( $\gamma$ ) on  $n$  and  $df$  was investigated and it was found that the best  $\gamma$  for Rose model is around 2.5 and for Mei model is around 6.

## ACKNOWLEDGMENTS

The authors are grateful to Nicolas Pionnier, Rémi Berger and Elise Contraires, for their help in taking experimental results. This work was supported by the LABEX MANUTECH-SISE (ANR-10-LABX-0075) from Ecole Centrale de Lyon, within the program "Investissements d'Avenir" (ANR-11-IDEX-0007) operated by the French National Research Agency (ANR).

## REFERENCES

- [1] Baojin Qi, Jinjia Wei, Li Zhang, and Hong Xu. A fractal dropwise condensation heat transfer model including the effects of contact angle and drop size distribution. *International Journal of Heat and Mass Transfer*, 83:259–272, 2015.
- [2] J.W. Rose E.J. Le Fevre. A theory of heat transfer by dropwise condensation. In *Proceedings of 3rd International Heat Transfer*, pages 362–375.
- [3] JW Rose and LR Glicksman. Dropwise condensation—the distribution of drop sizes. *International journal of heat and mass transfer*, 16(2):411–425, 1973.
- [4] Hfroaki Tanaka. A theoretical study of dropwise condensation. *ASME J. Heat Transfer*, 97(1):72–78, 1975.
- [5] Tsuruta Takaharu and Hiroaki Tanaka. A theoretical study on the constriction resistance in dropwise condensation. *International journal of heat and mass transfer*, 34(11):2779–2786, 1991.

- [6] Maofei Mei, Feng Hu, Chong Han, and Yanhai Cheng. Time-averaged droplet size distribution in steady-state dropwise condensation. *International Journal of Heat and Mass Transfer*, 88:338–345, 2015.
- [7] Maofei Mei, Boming Yu, Jianchao Cai, and Liang Luo. A fractal analysis of dropwise condensation heat transfer. *International Journal of Heat and Mass Transfer*, 52(21):4823–4828, 2009.
- [8] Yu-Ting Wu, Chun-Xin Yang, and Xiu-Gan Yuan. Drop distributions and numerical simulation of dropwise condensation heat transfer. *International Journal of Heat and Mass Transfer*, 44(23):4455–4464, 2001.
- [9] Noriyuki Watanabe, Masanori Aritomi, and Atsumi Machida. Time-series characteristics and geometric structures of drop-size distribution density in dropwise condensation. *International Journal of Heat and Mass Transfer*, 76:467–483, 2014.
- [10] Clark Graham and Peter Griffith. Drop size distributions and heat transfer in dropwise condensation. *International Journal of Heat and Mass Transfer*, 16(2):337–346, 1973.
- [11] H Tanaka. Measurements of drop-size distributions during transient dropwise condensation. *Journal of Heat Transfer*, 97(3):341–346, 1975.
- [12] JW Rose. Dropwise condensation theory and experiment: a review. *Proceedings of the Institution of Mechanical Engineers, Part A: Journal of Power and Energy*, 216(2):115–128, 2002.
- [13] Martin Churchill. Introduction to fractal geometry. *Keble Summer Essay*, 2004.
- [14] JW Rose. Dropwise condensation theory. *International Journal of Heat and Mass Transfer*, 24(2):191–194, 1981.
- [15] Mousa Abu-Orabi. Modeling of heat transfer in dropwise condensation. *International journal of heat and mass transfer*, 41(1):81–87, 1998.
- [16] Maofei Mei, Boming Yu, Mingqing Zou, and Liang Luo. A numerical study on growth mechanism of dropwise condensation. *International Journal of Heat and Mass Transfer*, 54(9):2004–2013, 2011.
- [17] P Meakin. Dropwise condensation: the deposition growth and coalescence of fluid droplets. *Physica Scripta*, 1992(T44):31, 1992.
- [18] John Francis Welch. *Microscopic study of dropwise condensation*. PhD thesis, University of Illinois at Urbana-Champaign, 1961.